引用格式：WANG Yu, TIAN Yiqian, JIANG Haoyu, et al. Remodeling of the Localized Approximation: Beam Shape Coefficient Calculation for the Gaussian Beam by Using Scalar Translation Addition Theorem[J]. Acta Photonica Sinica, 2026, 55(3): 0326002
王裕，田艺茜，江浩宇，等. 局域近似法的光束重构：高斯光束形状系数的标量平移计算方法[J]. 光子学报，2026，55(3)：0326002

局域近似法的光束重构：高斯光束形状系数的标量平移计算方法

王裕，田艺茜，江浩宇，沈建琪
（上海理工大学 理学院，上海 200093）

摘　要：采用两步间接法结合局域近似法计算有形光束电磁场的光束形状系数，并讨论了两步间接法结合局域近似法和直接采用局域近似法重构高斯光束之间的差异。该方法首先采用标量势函数描述在轴时的结构光束，利用标量平移定理及标量势函数与电磁场之间的关系得到离轴时的矢量光束形状系数。采用两步间接法计算有形光束的光束形状系数，不仅简化了光束形状系数的表述，还加快了数值计算的速度。高斯光束的数值计算结果验证了该方法在计算光束形状系数和进行场重构上有较好的精度和效率。

关键词：光束形状系数；标量加法定理；局域近似法；高斯光束；光束重构
中图分类号：O436.2　　**文献标识码**：A　　**doi**：10.3788/gzxb20265503.0326002

0 引言

在研究球形颗粒与结构光束相互作用时，光束的电磁场被展开为矢量球谐函数的无穷级数，级数的权重系数称作光束形状系数(Beam Shape Coefficient, BSC)[1]。准确且高效地计算光束形状系数对于研究光束与粒子的相互作用至关重要。在过去几十年里已经发展了多种不同的方法，如正交法[2,3]、局域近似法[4-6]、有限级数法[7-9]和角谱分解法[10-12]等。在正交法中，光束形状系数的数值计算涉及二重或三重积分。由于被积函数的强振荡特性，正交法的数值计算往往耗时颇多。在采用角谱法计算光束形状系数时，也需要执行积分运算。尽管其运算速度与正交法相比有较大提升，但同样较慢。在有限级数法和局域近似法中，光束形状系数通常以级数形式表示，这使得它们在计算效率上更具优势。然而，有限级数法在公式推导方面比较复杂，迄今为止主要针对在轴光束[7,8,13-15]；而且在光束形状系数的高阶项中由于有效位数的丢失使得其计算结果出现严重偏差[15]。局域近似法具有公式推导简单、适用于在轴和离轴光束、运算速度快且收敛良好等优势，因此得到了广泛应用。然而，局域近似法基于范德赫尔斯特(van de Hulst)的局域原理[16]，将照射到颗粒上的电磁波看成一系列局域几何光束。因此，局域近似法属于一种近似计算方法，它对入射光的电磁场进行了重构。最近的研究表明，对于强会聚光束或光束带有锥角或拓扑荷时，局域近似法会带来较大的误差[9,12,17-23]。与原始场进行数值比较发现，在局域近似法的重构场中易出现伪峰，且当光束离轴距离较大时伪峰呈环状结构[24-29]。

迄今为止，对局域近似法的场重构效应研究相对比较零散且尚未深入。本文基于一种近期提出的两步间接法对此开展研究[30]。该方法首先采用标量势函数描述结构光束，在光束坐标系中进行球谐函数级数展开，得到光束坐标系中的标量光束形状系数。然后利用标量平移定理，得到颗粒坐标系中的光束形状系数。

第一作者：王裕，1527231855@qq.com
通讯作者：沈建琪，jqshenk@usst.edu.cn
收稿日期：2025-10-17；**录用日期**：2025-11-18

最后构建标量势函数与电磁场的关系，得到颗粒坐标系中电磁场的级数展开式及其光束形状系数。研究表明，两步间接法具有理论推导简单且数值计算快速的优势。首先，在光束坐标系中光束中心位于坐标原点，故光束形状系数易推导且表达式简单，其数值计算快速高效。其次，在标量波的球谐函数级数展开式中只涉及一组权重系数，而在电磁场的展开式中电场和磁场分别对应一组权重系数，故采用标量波的形式使理论推导和数值计算减少了一半工作量[31]。因此，采用两步间接法计算光束形状系数使得理论分析简单和数值计算高效。

文献[30]采用了角谱法计算光束坐标系中标量波的光束形状系数。本文将采用局域近似法替代角谱法，研究两步间接法中局域近似对高斯光束的重构效应，并与直接法中的光束重构进行比较分析。

1 理论

如图1所示，沿z_1轴传播的高斯光束其束腰中心位于坐标系1(光束坐标系)原点，球形颗粒的中心位于坐标系2(颗粒坐标系)原点。矢量$\boldsymbol{r}_1$和$\boldsymbol{r}_2$分别表示场点P在光束系和颗粒系中的坐标，则两个坐标系的关系可用矢量$\boldsymbol{r}_{12}=\boldsymbol{r}_1-\boldsymbol{r}_2$(或$\boldsymbol{r}_0=-\boldsymbol{r}_{12}$)表示，$\boldsymbol{r}_{12}$从$o_1$指向$o_2$。

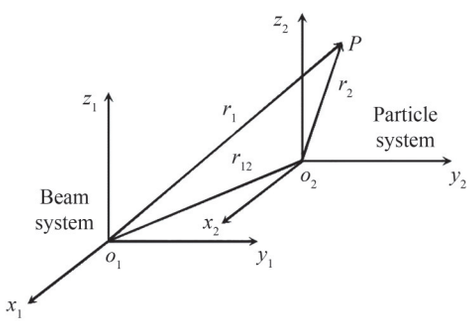

图1 光束系和颗粒系的几何关系

Fig.1 Geometric relation between the beam and particle systems

1.1 标量平移定理

根据电磁场理论[32]，满足亥姆霍兹方程$\nabla^2\psi(\boldsymbol{r}_j)+k^2\psi(\boldsymbol{r}_j)=0$的标量势函数$\psi(\boldsymbol{r}_j)$在球坐标系中可展开为球谐函数$\psi_{nm}(\boldsymbol{r}_j)$的级数形式

$$\psi(\boldsymbol{r}_j)=\sum_{n=0}^{\infty}\sum_{m=-n}^{+n}g_{nm}^{(j)}\psi_{nm}(\boldsymbol{r}_j) \tag{1}$$

$$\psi_{nm}(\boldsymbol{r}_j)=j_n(R_j)\tilde{P}_n^m(\cos\theta_j)\exp(\mathrm{i}m\varphi_j) \tag{2}$$

式中，角标$j=1,2$分别指代光束系和颗粒系，$R_j=kr_j$是无因次径向变量，$k=2\pi/\lambda$是波矢常数，λ是波长。注意，式(1)中的权重系数$g_{nm}^{(j)}$称作标量光束形状系数，与归一化缔合勒让德函数$\tilde{P}_n^m(\cos\theta_j)$对应。

根据标量平移定理[33-36]，两个坐标系中的球谐函数满足关系

$$\psi_{\nu\mu}(\boldsymbol{r}_1)=\sum_{n=0}^{\infty}\sum_{m=-n}^{+n}\beta_{nm}^{\nu\mu}(\boldsymbol{r}_{12})\psi_{nm}(\boldsymbol{r}_2) \tag{3}$$

式中，$\beta_{nm}^{\nu\mu}(\boldsymbol{r}_{12})$是平移系数，与矢量$\boldsymbol{r}_{12}$的大小和方向有关。平移系数$\beta_{nm}^{\nu\mu}(\boldsymbol{r}_{12})$的定义及其迭代计算公式详见文献[30]，此处从略。将式(3)和式(1)结合即可得到两个坐标系中标量光束形状系数的关系

$$g_{nm}^{(2)}=\sum_{\nu=0}^{\infty}\sum_{\mu=-\nu}^{+\nu}\beta_{nm}^{\nu\mu}(\boldsymbol{r}_{12})g_{\nu\mu}^{(1)} \tag{4}$$

对于弱会聚的高斯光束，标量势函数在光束坐标系中可采用傍轴近似式表示

$$\psi(\boldsymbol{r}_1)=Q\exp\left(-Q\rho_1^2/w_0^2\right)\exp(\mathrm{i}kz_1) \tag{5}$$

式中，$Q=\left(1+\mathrm{i}2z_1k^{-1}w_0^{-2}\right)^{-1}$，$\rho_1=\left(x_1^2+y_1^2\right)^{1/2}$代表场点在$xy$平面内的径向变量，$w_0$是高斯光束的束腰半径。标量势函数在颗粒坐标系中的表达式$\psi(\boldsymbol{r}_2)$可以通过坐标变换$\boldsymbol{r}_2=\boldsymbol{r}_1+\boldsymbol{r}_0$从式(5)得到。

由文献[37]可知，$g_{nm}^{(2)}$的局域近似表达式为

$$g_{nm}^{(2)}=2\mathrm{i}^{n-m}(n+0.5)^{1/2-|m|}\sqrt{\frac{(n+|m|)!}{(n-|m|)!}}\,\bar{Q}\mathrm{e}^{-\mathrm{i}kz_0-\mathrm{i}m\phi_0-\bar{Q}s^2(R_n^2+k^2\rho_0^2)}I_m\left(2\bar{Q}s^2R_nk\rho_0\right)\tag{6}$$

式中，(ρ_0,ϕ_0,z_0)是$\boldsymbol{r}_0$的柱坐标分量，$R_n=n+0.5$、$\bar{Q}=(1-\mathrm{i}2s^2kz_0)^{-1}$和$s=(kw_0)^{-1}$均为无因次参量。

从式(6)可以看出，当n增大时光束形状系数$g_{nm}^{(2)}$按照指数方式递减；随着$|m|$增大$g_{nm}^{(2)}$的值也快速减小。因此，在颗粒坐标系中(即$j=2$)，式(1)的双重求和可根据w_0(或s)的具体大小选取适当的截止数$n_{\max}$和$m_{\max}$。这表示在颗粒系中需计算大约$(n_{\max}+1)\times(2m_{\max}+1)$个$g_{nm}^{(2)}$的值。

式(6)中令$\boldsymbol{r}_0=0$，并用角标ν和μ分别替换n和m，则可得到

$$g_{\nu\mu}^{(1)}=\delta_{\mu,0}2\mathrm{i}^{\nu}(\nu+0.5)^{1/2}\exp(-s^2R_\nu^2)\tag{7}$$

式中，$R_\nu=\nu+0.5$。由于$g_{\nu\mu}^{(1)}$仅在$\mu=0$时才有非零值，且随着ν增大$g_{\nu\mu}^{(1)}$的值以指数方式递减，因此只需计算$\nu=0\rightarrow\nu_{\max}$(即$\nu_{\max}+1$个)光束形状系数。比较式(6)和式(7)不难发现，$g_{\nu\mu}^{(1)}$的表达式比$g_{nm}^{(2)}$简单得多，而且只需要计算$\nu_{\max}+1$个$g_{\nu\mu}^{(1)}$。因此，在光束系中光束形状系数的计算更快。在式(4)的平移计算公式中，双重求和退化为单重求和。

$$g_{nm}^{(2)}=\sum_{\nu=0}^{\nu_{\max}}\beta_{nm}^{\nu,0}(\boldsymbol{r}_{12})\,g_{\nu,0}^{(1)}\tag{8}$$

1.2 标量光束形状系数与矢量光束形状系数

根据麦克斯韦电磁场理论，在洛伦兹规范下光束的电场$\boldsymbol{E}(\boldsymbol{r}_j)$满足亥姆霍兹方程$\nabla^2\boldsymbol{E}(\boldsymbol{r}_j)+k^2\boldsymbol{E}(\boldsymbol{r}_j)=0$和散度条件$\nabla\cdot\boldsymbol{E}(\boldsymbol{r}_j)=0$，可以表示为[32,38]

$$\boldsymbol{E}(\boldsymbol{r}_j)=\frac{1}{2}\left[k^{-2}\nabla\times\nabla\times\boldsymbol{A}(\boldsymbol{r}_j)+\mathrm{i}k^{-1}\nabla\times\boldsymbol{A}^*(\boldsymbol{r}_j)\right]\tag{9}$$

式(9)对应时谐项$\exp(-\mathrm{i}\omega t)$，其中$\omega$为角频率。对于沿$z$轴方向传播的光束，矢势$\boldsymbol{A}(\boldsymbol{r}_j)$和$\boldsymbol{A}^*(\boldsymbol{r}_j)$由式(10)给出。

$$\begin{cases}\boldsymbol{A}(\boldsymbol{r}_j)=(p_x\boldsymbol{e}_x+p_y\boldsymbol{e}_y)\psi(\boldsymbol{r}_j)\\ \boldsymbol{A}^*(\boldsymbol{r}_j)=\boldsymbol{e}_z\times\boldsymbol{A}(\boldsymbol{r}_j)=(p_x\boldsymbol{e}_y-p_y\boldsymbol{e}_x)\psi(\boldsymbol{r}_j)\end{cases}\tag{10}$$

式中，$\psi(\boldsymbol{r}_2)$是标量势函数，(p_x,p_y)是偏振参量。电场$\boldsymbol{E}(\boldsymbol{r}_j)$的球谐函数级数展开式为

$$\boldsymbol{E}(\boldsymbol{r}_j)=\sum_{n=1}^{\infty}\sum_{m=-n}^{+n}\left\{G_{nm}^{\mathrm{TE},j}\boldsymbol{M}_{n,m}^{(1)}(\boldsymbol{r}_j)+G_{nm}^{\mathrm{TM},j}\boldsymbol{N}_{n,m}^{(1)}(\boldsymbol{r}_j)\right\}\tag{11}$$

相应的磁场满足关系式$\boldsymbol{H}(\boldsymbol{r}_j)=(\mathrm{i}\mu\omega)^{-1}\nabla\times\boldsymbol{E}(\boldsymbol{r}_j)$，其中$\mu$为磁导率。利用$\nabla\times\boldsymbol{M}_{nm}^{(1)}=k\boldsymbol{N}_{nm}^{(1)}$和$\nabla\times\boldsymbol{N}_{nm}^{(1)}=k\boldsymbol{M}_{nm}^{(1)}$[32]，由式(11)可得到磁场的级数展开式，表示为

$$\boldsymbol{H}(\boldsymbol{r}_j)=(\mathrm{i}\mu\omega)^{-1}k\sum_{n=1}^{\infty}\sum_{m=-n}^{+n}\left\{G_{nm}^{\mathrm{TE},j}\boldsymbol{N}_{n,m}^{(1)}(\boldsymbol{r}_j)+G_{nm}^{\mathrm{TM},j}\boldsymbol{M}_{n,m}^{(1)}(\boldsymbol{r}_j)\right\}\tag{12}$$

式中，球谐函数$\boldsymbol{M}_{n,m}^{(1)}(\boldsymbol{r}_j)$和$\boldsymbol{N}_{n,m}^{(1)}(\boldsymbol{r}_j)$的具体表达式参见文献[30]。

电磁场级数展开式中的权重系数$(G_{nm}^{\mathrm{TE},j},G_{nm}^{\mathrm{TM},j})$称作矢量光束形状系数，其中角标TE和TM分别表示横电波(transverse electric wave)和横磁波(transverse magnetic wave)。根据文献[31, 39]，$(G_{nm}^{\mathrm{TE},j},G_{nm}^{\mathrm{TM},j})$可以表示为$g_{nm}^{(j)}$的线性组合。

$$\begin{pmatrix}G_{nm}^{\mathrm{TE},j}\\ G_{nm}^{\mathrm{TM},j}\end{pmatrix}=-p_-\left(\mathrm{i}C_1^-g_{n,m-1}^{(j)}+C_2^-g_{n+1,m-1}^{(j)}-C_3^-g_{n-1,m-1}^{(j)}\right)\mp p_+\left(\mathrm{i}C_1^+g_{n,m+1}^{(j)}+C_2^+g_{n+1,m+1}^{(j)}-C_3^+g_{n-1,m+1}^{(j)}\right)\tag{13}$$

式中，$p_\pm=p_x\pm\mathrm{i}p_y$，系数$C_i^\pm$分别为

$$\begin{cases} C_1^{\pm}=\dfrac{1}{4n(n+1)}\sqrt{(n\mp m)(n\pm m+1)} \\ C_2^{\pm}=\dfrac{1}{4(n+1)}\sqrt{\dfrac{(n\pm m+1)(n\pm m+2)}{(2n+1)(2n+3)}} \\ C_3^{\pm}=\dfrac{1}{4n}\sqrt{\dfrac{(n\mp m)(n\mp m-1)}{(2n-1)(2n+1)}} \end{cases} \tag{14}$$

式(13)和式(14)给出了$\left(G_{nm}^{\mathrm{TE},j},G_{nm}^{\mathrm{TM},j}\right)$的间接计算公式,其中$j=1,2$,表示该间接计算公式对光束系和颗粒系均适用。此外,光束形状系数$\left(G_{nm}^{\mathrm{TE},j},G_{nm}^{\mathrm{TM},j}\right)$也可以直接求解。为此,将式(10)代入式(9)并作傍轴近似,得到电磁场的近似表达式

$$\begin{cases} \boldsymbol{E}(\boldsymbol{r}_j)=\left(p_x\boldsymbol{e}_x+p_y\boldsymbol{e}_y\right)\psi(\boldsymbol{r}_j) \\ \boldsymbol{H}(\boldsymbol{r}_j)=\left(p_x\boldsymbol{e}_y-p_y\boldsymbol{e}_x\right)k(\mu\omega)^{-1}\psi(\boldsymbol{r}_j) \end{cases} \tag{15}$$

在颗粒坐标系中取$j=2$,标量函数$\psi(\boldsymbol{r}_2)$从式(5)给出的$\psi(\boldsymbol{r}_1)$通过坐标变换得到。利用广义米理论的局域近似法[4, 27]即可得到颗粒系中$\left(G_{nm}^{\mathrm{TE},2},G_{nm}^{\mathrm{TM},2}\right)$的表达式

$$\begin{aligned} \begin{pmatrix} G_{nm}^{\mathrm{TE},2} \\ G_{nm}^{\mathrm{TM},2} \end{pmatrix}=&\mathrm{i}^{n-m}\frac{(n+0.5)^{3/2-|m|}}{n(n+1)}\sqrt{\frac{(n+|m|)!}{(n-|m|)!}}\,\bar{Q}\exp\left[-\bar{Q}\left(R_n^2+k^2\rho_0^2\right)s^2-\mathrm{i}kz_0\right]\times \\ &\left\{p_-\mathrm{e}^{-\mathrm{i}(m-1)\phi_0}I_{m-1}\left(2\bar{Q}s^2k\rho_0R_n\right)\mp p_+\mathrm{e}^{-\mathrm{i}(m+1)\phi_0}I_{m+1}\left(2\bar{Q}s^2k\rho_0R_n\right)\right\} \end{aligned} \tag{16}$$

式中,令$\boldsymbol{r}_0=0$,并用角标ν和μ分别替换n和m,即可得到光束坐标系中的表达式

$$\begin{pmatrix} G_{\nu\mu}^{\mathrm{TE},1} \\ G_{\nu\mu}^{\mathrm{TM},1} \end{pmatrix}=\left(\delta_{\mu,1}p_-\pm\delta_{\mu,-1}p_+\right)\mathrm{i}^{\nu-1}\left[\frac{\nu+0.5}{\nu(\nu+1)}\right]^{1/2}\exp\left(-R_\nu^2s^2\right) \tag{17}$$

式中,$R_\nu=\nu+0.5$。

值得注意的是,式(16)也可以通过将式(6)代入式(13)得到,同理将式(7)代入式(13)可得到式(17)。

2 数值计算与讨论

2.1 光束形状系数

作为示例,图2给出了参数为$w_0=3\ \mu\mathrm{m}$、$\lambda=0.632\,8\ \mu\mathrm{m}$,$(x_0,y_0,z_0)=(2,2,0)\ \mu\mathrm{m}$和$(p_x,p_y)=(1,0)$时采用局域近似法计算光束形状系数$G_{nm}^{\mathrm{TM},2}$的结果。其中,图2(a)采用双精度通过式(16)直接计算,用角标dir表示;图2(b)采用双精度间接计算方法,首先通过式(7)计算$g_{\nu,0}^{(1)}$,然后利用式(8)进行平移处理得到$g_{nm}^{(2)}$,最后采用式(13)得到$G_{nm}^{\mathrm{TM},2}$,用角标DP表示双精度(double precision);图2(c)的计算方法与图2(b)一致,但在平移计算时平移系数$\beta_{nm}^{\nu\mu}(\boldsymbol{r}_{12})$采用了Mathematica的十进制1 000位的高精度算法,用角标HP表示高精度(high precision)。从图2(a)可以看出,直接法得到的$G_{nm}^{\mathrm{TM},2}$分布比较规则,而图2(b)的双精度间接法计算结果在$m>30$的区域内出现了不规则分布。采用高精度所得到的图2(c)间接法计算结果的分布比图2(b)更加规则。

图2(d)~(f)分别给出了各种计算方法计算所得到的矢量光束形状系数$G_{nm}^{\mathrm{TM},2}$之差,定义为$\Delta\left|G_{nm}^{\mathrm{TM},2}\right|=\left|G_{nm,i}^{\mathrm{TM},2}-G_{nm,j}^{\mathrm{TM},2}\right|$。其中角标$i$和$j$可以是dir、DP和HP中任意二个,它们依次代表直接算法、双精度间接算法和高精度间接算法。为简洁起见,图2(d)~(f)中光束形状系数的角标只保留了dir、DP和HP。图2(d)给出了直接算法和双精度间接算法所得到的$G_{nm}^{\mathrm{TM},2}$的差值,可以发现两种方法的区别主要出现在$m\leqslant20$的区域,最大达到了约$\Delta\left|G_{nm}^{\mathrm{TM},2}\right|=4.2\times10^{-5}$。在$m>20$的区域分布不太规则但$\Delta\left|G_{nm}^{\mathrm{TM},2}\right|$的值较小,$\Delta\left|G_{nm}^{\mathrm{TM},2}\right|<5\times10^{-18}$;图2(e)比较了直接算法和高精度间接算法所得$G_{nm}^{\mathrm{TM},2}$的差值,在$m\leqslant20$范围内的情况与图2(d)类似,但在$m>20$的区域内$\Delta\left|G_{nm}^{\mathrm{TM},2}\right|$的分布比较规则且数值比图2(d)中更小,$\Delta\left|G_{nm}^{\mathrm{TM},2}\right|<2.2\times10^{-18}$。图2(f)比较了两种精度的间接算法所得$G_{nm}^{\mathrm{TM},2}$的差值。从图中可以看出,在整个计算范围内,两者之差总体较小,$\Delta\left|G_{nm}^{\mathrm{TM},2}\right|<1.0\times10^{-15}$。这说明高精度计算对$G_{nm}^{\mathrm{TM},2}$的计算结果有一定的效果,但并不明显。

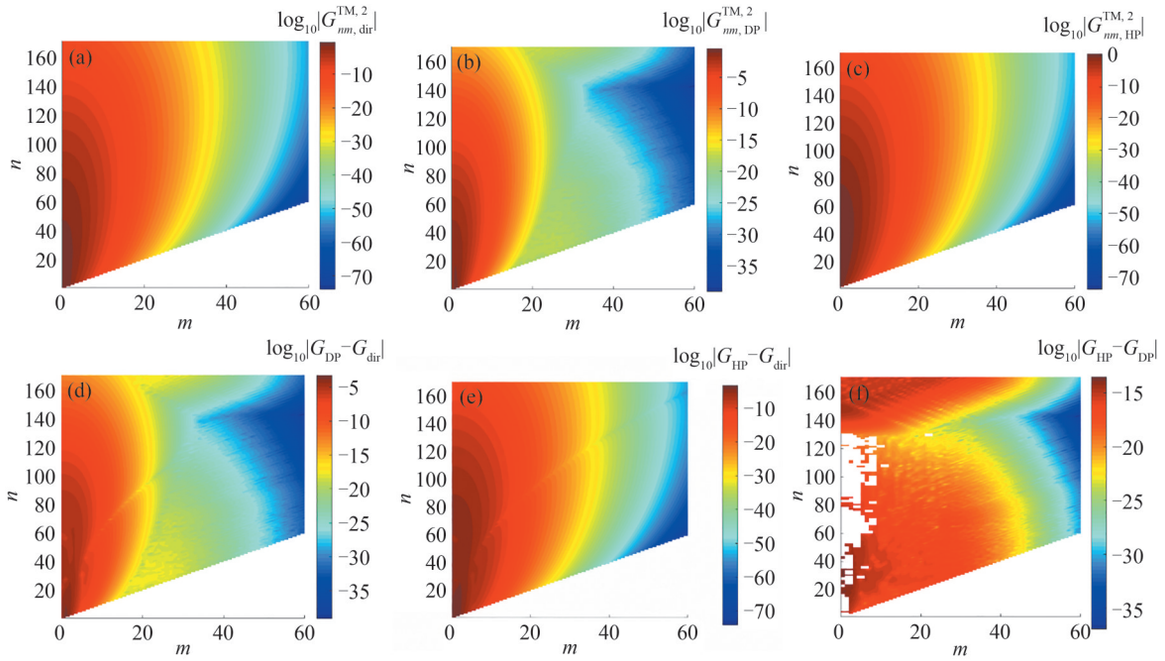

图2　直接法和间接法得到的光束形状系数 $G_{nm}^{TM,2}$ 计算结果比较。(a)直接法；(b)双精度间接法；(c)高精度间接法；(d)直接法与双精度间接法之差；(e)直接法与高精度间接法之差；(f)双精度与高精度间接法之差

Fig. 2　Numerical results of the vector BSCs $G_{nm}^{TM,2}$ and the comparison. (a) Direct method; (b) Indirect method with DP; (c) Indirect method with HP; (d) Difference between direct and DP indirect method; (e) Difference between direct and HP indirect method; (f) Difference between DP and HP indirect methods

图3给出了双精度计算得到的 $\Delta|G_{nm}^{TM,2}|$ 在 $m=0$ 时随 n 的变化曲线和 $\Delta|G_{nm}^{TM,2}|$ 在 $n=60$ 时随 m 的变化情况，其中图3(b)还给出了曲线的对数坐标曲线。可以看出，两条曲线的最大值分别达到了 $\Delta|G_{nm}^{TM,2}|=4.2\times10^{-5}$ 和 1.3×10^{-5}。造成该现象的主要原因来自两个方面。其中一个原因是局域近似法对光束结构的重构。首先，式(5)给出的高斯光束并不满足亥姆霍兹方程，但是式(1)的球函数级数展开则严格满足亥姆霍兹方程。因此，在对光束进行球函数级数展开的过程中光束进行了重构。其次，由于局域法属于一种近似计算方法，故在局域近似过程中还存在对光束结构的重构。局域法的重构效应与光束的半径以及光束中心在坐标系中的位置有关。在间接法中光束重构时光束中心位于坐标原点，而在直接法中光束中心在 (x_0,x_0,z_0) 处，这是导致两种方法所得结果不同的原因之一。另一个可能的原因是在平移过程中由于平移系数 $\beta_{nm}^{\nu\mu}(\boldsymbol{r}_{12})$ 的计算误差所导致的差异。但是，从图2(f)可以看到，即使采用了高精度计算遏制平移系数

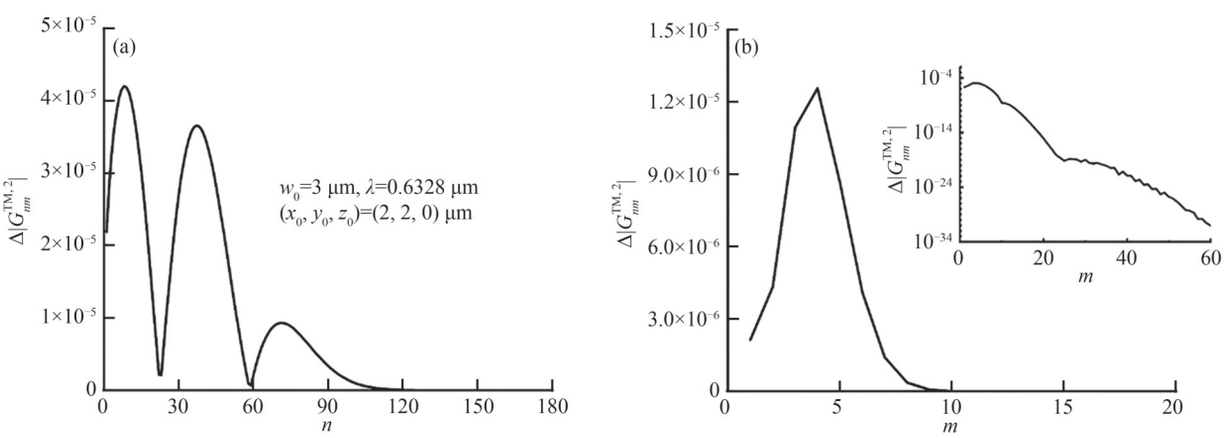

图3　直接法和间接法光束形状系数 $G_{nm}^{TM,2}$ 之间的偏差。(a)不同分波 n；(b)不同方位角模式 m

Fig. 3　Difference between the vector BSCs $G_{nm}^{TM,2}$ calculated with direct and indirect methods. (a) with variant partial waves; (b) with variant azimuthal modes

$\beta_{nm}^{\nu\mu}(\boldsymbol{r}_{12})$的计算误差，对$\Delta\left|G_{nm}^{\mathrm{TM},2}\right|$的作用也是有限的。这表明，平移系数$\beta_{nm}^{\nu\mu}(\boldsymbol{r}_{12})$所引入的误差非常小。因此，直接算法和间接算法所得结果之差主要归结于局域近似法的重构效应。

采用双精度C代码在i7 CPU @ 2.60 GHz个人电脑上计算光束形状系数，直接算法和间接算法的速度比较如表1。第一列为光束中心离轴位置$\boldsymbol{r}_{12}$的直角坐标，第二至第四列分别给出计算$g_{\nu,0}^{(1)}$、从$g_{\nu,0}^{(1)}$向$g_{nm}^{(2)}$的平移(用B-to-P表示)以及从$g_{nm}^{(2)}$转化为$\left(G_{nm}^{\mathrm{TE},2}, G_{nm}^{\mathrm{TM},2}\right)$的计算时间(用S-to-V表示)，间接方法总耗时在第五列给出。最后两列分别是直接算法计算$g_{nm}^{(2)}$和$\left(G_{nm}^{\mathrm{TE},2}, G_{nm}^{\mathrm{TM},2}\right)$的耗时。考虑到光束形状系数在$|m|>20$时的值很小，故计算范围设定为$n\leqslant 172$、$|m|\leqslant 20$。可以看出，局域法计算$g_{\nu,0}^{(1)}$耗时一般少于0.3 s，从$g_{\nu,0}^{(1)}$向$g_{nm}^{(2)}$平移转换约需0.1s，从$g_{nm}^{(2)}$向$\left(G_{nm}^{\mathrm{TE},2}, G_{nm}^{\mathrm{TM},2}\right)$的转换仅需约20 ms。间接法计算$\left(G_{nm}^{\mathrm{TE},2}, G_{nm}^{\mathrm{TM},2}\right)$的总耗时不足1 s。而采用直接法计算$\left(G_{nm}^{\mathrm{TE},2}, G_{nm}^{\mathrm{TM},2}\right)$至少需约8 s。光束中心的离轴位置$\boldsymbol{r}_{12}$增大时，计算耗时稍有增加，但差别不大。显然，间接法比直接法在计算效率上高得多。

表1 比较光束形状系数的计算时间

Table1 Comparison of CPU time for BSC calculation

$\boldsymbol{r}_{12}(x_{12}, y_{12}, z_{12})$	$g_{n,0}^{(1)}$	B-to-P	S-to-V	Indirect method	Direct method	
					$g_{nm}^{(2)}$	$\left(G_{nm}^{\mathrm{TE},2}, G_{nm}^{\mathrm{TM},2}\right)$
(0, 2, 0)	0.224	0.097	0.017	0.338	1.338	7.896
(3, 0, 0)	0.242	0.098	0.017	0.357	1.359	8.783
(2, 2, 5)	0.237	0.094	0.017	0.347	1.350	9.418
(3, 4, −10)	0.381	0.138	0.022	0.541	1.583	12.69

* The units in the first column are μm, while the units in the other columns are seconds. B-to-P means translation from beam coordinates to particle coordinates, and S-to-V means the transform from scalar BSCs to the vector ones

2.2 电场重构

分别采用直接法和间接计算法得到光束形状系数$\left(G_{nm}^{\mathrm{TE},2}, G_{nm}^{\mathrm{TM},2}\right)$，通过式(11)计算高斯光束在$xy$平面内的电场分布，如图4所示，其中参数为$w_0=3\ \mu\mathrm{m}$、$\lambda=0.6328\ \mu\mathrm{m}$和$(x_0, y_0, z_0)=(2, 2, 0)\ \mu\mathrm{m}$。其中图4(a)是采用直接法光束形状系数重构得到的电场分布，用角标dir表示直接法。可以看出，大于$|\boldsymbol{E}|\geqslant 10^{-7}$的电场得到了重构，而场强较弱的区域没有重构成功。其部分原因是式(11)对n和m求和时采取了截止数$n_{\max}=171$和$m_{\max}=50$，另一部分源于光束形状系数的计算方法。图4(b)是采用间接法光束形状系数重构得到的电场分布，用角标ind表示间接法。可以看出，$|\boldsymbol{E}|\geqslant 10^{-13}$的场可以得到重构，这比直接法低了6个数量级。图4(c)和(d)分别是两种方法得到的重构场与原始场之差$\Delta|\boldsymbol{E}|=|\boldsymbol{E}_i-\boldsymbol{E}_{\mathrm{asr}}|$。这里原始场采用文献[30]中的角谱表达式进行计算，用角标asr表示。角标$i=$dir, ind代表重构场的计算方法。在图4(c)中重构场与原始场之差最大达$\Delta|\boldsymbol{E}|\approx 8.75\times 10^{-4}$，而在图4(d)中为$\Delta|\boldsymbol{E}|\approx 6.69\times 10^{-4}$。这表明，相较于直接法，间接法的重构场与原始场更接近。

图5～图7分别给出了$x_0=4\ \mu\mathrm{m}$、$x_0=6\ \mu\mathrm{m}$和$x_0=8\ \mu\mathrm{m}$的重构场比较，其余参数不变。计算发现，直接法得到的重构场与光束离轴距离的关系很明显。与$x_0=4\ \mu\mathrm{m}$、$6\ \mu\mathrm{m}$和$8\ \mu\mathrm{m}$相对应，重构场与原始场之差最大值分别为$\Delta|\boldsymbol{E}|\approx 1.15\times 10^{-3}$、$1.92\times 10^{-3}$和$2.79\times 10^{-3}$。这说明，随着光束离轴距离增大，直接法重构场与原始场之间的差别越来越明显。比较图4(a)、5(a)、6(a)和7(a)可以发现，随着光束离轴距离增大，重构场中靠近坐标原点的一侧出现了一个鼓包(也称作伪峰)，其高度约为$|\boldsymbol{E}|\approx 10^{-5}$。这表明，直接法得到的重构场分布偏离了高斯光束的轴对称结构。从图7(a)可以看出，当$x_0=8\ \mu\mathrm{m}$时，该伪峰演变成一个以坐标原点为中心的环状结构。直接法重构场的这种变化规律与文献[24, 27, 28]中的计算结果吻合。

与上述情况相反，从图4(b)、5(b)、6(b)和7(b)中可以看出，间接法重构场始终保持高斯光束的轴对称分布。间接法重构场与光束离轴距离的关联性不强，仅在场强较弱区域有明显的变化，这与平移系数$\beta_{nm}^{\nu\mu}(\boldsymbol{r}_{12})$在$\nu>n$时的计算误差有关。此外，从图4(d)、5(d)、6(d)和7(d)中可以发现，重构场与原始场之差的最大值始终保持在$\Delta|\boldsymbol{E}|\approx 6.69\times 10^{-4}$。实际上，在间接计算方法中，重构场与原始场之差与光束中心位

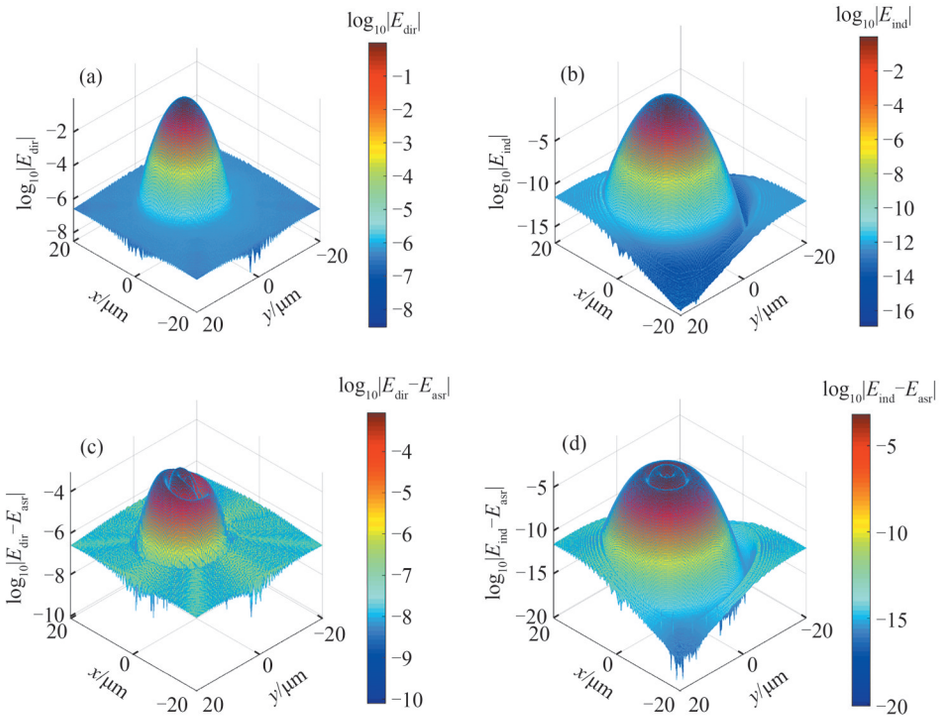

图4　高斯光束的重构场及其偏差，光束中心位于$(x_0, y_0, z_0)=(2, 2, 0)$ μm。(a)直接法重构电场；(b)间接法重构电场；(c)直接法重构误差；(d)间接法重构误差

Fig. 4　Reconstructed electric fields of the Gaussian beam centered at .$(x_0, y_0, z_0)=(2, 2, 0)$ μm. (a) Electric field reconstructed in direct method; (b) Electric field reconstructed in indirect method; (c) Difference between the original and directly reconstructed fields; (d) Difference between the original and indirectly reconstructed fields

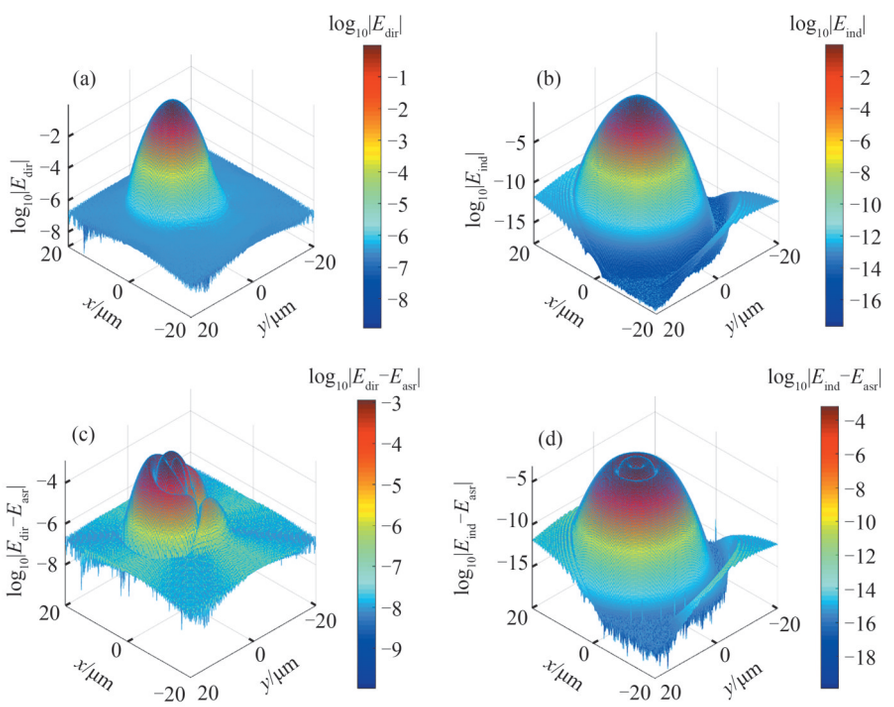

图5　高斯光束的重构场及其偏差，光束中心位于$(x_0, y_0, z_0)=(4, 2, 0)$ μm。(a)直接法重构电场；(b)间接法重构电场；(c)直接法重构误差；(d)间接法重构误差

Fig. 5　Reconstructed electric fields of the Gaussian beam centered at $(x_0, y_0, z_0)=(4, 2, 0)$ μm. (a) Electric field reconstructed in direct method; (b) Electric field reconstructed in indirect method; (c) Difference between the original and directly reconstructed fields; (d) Difference between the original and indirectly reconstructed fields

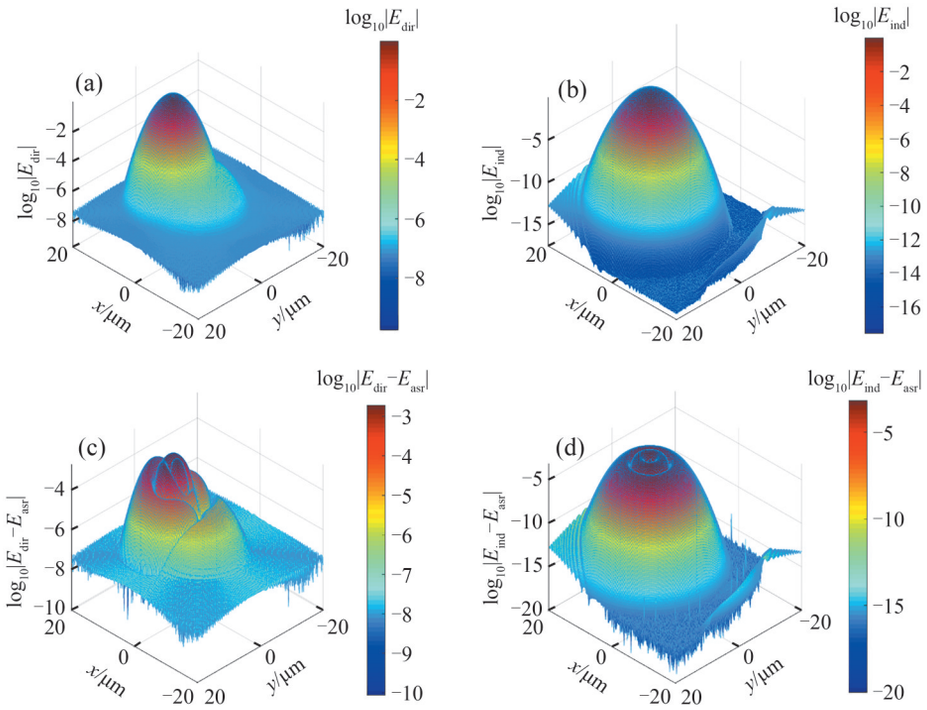

图 6 高斯光束的重构场及其偏差，光束中心位于$(x_0, y_0, z_0)=(6, 2, 0)$ μm。(a)直接法重构电场；(b)间接法重构电场；(c)直接法重构误差；(d)间接法重构误差

Fig. 6 Reconstructed electric fields of the Gaussian beam centered at $(x_0, y_0, z_0)=(6, 2, 0)$ μm. (a) Electric field reconstructed in direct method; (b) Electric field reconstructed in indirect method; (c) Difference between the original and directly reconstructed fields; (d) Difference between the original and indirectly reconstructed fields

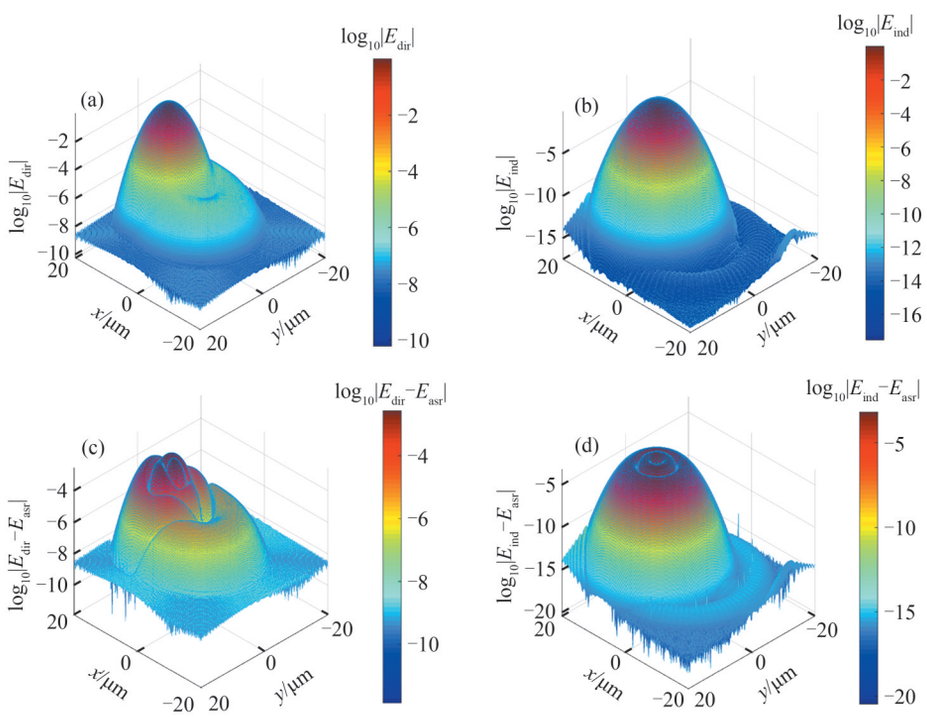

图 7 高斯光束的重构场及其偏差，光束中心位于$(x_0, y_0, z_0)=(8, 2, 0)$ μm。(a)直接法重构电场；(b)间接法重构电场；(c)直接法重构误差；(d)间接法重构误差

Fig. 7 Reconstructed electric fields of the Gaussian beam centered at $(x_0, y_0, z_0)=(8, 2, 0)$ μm. (a) Electric field reconstructed in direct method; (b) Electric field reconstructed in indirect method; (c) Difference between the original and directly reconstructed fields; (d) Difference between the original and indirectly reconstructed fields

于坐标原点时的情况完全一致。光束形状系数的平移计算对重构场并不产生明显的影响，这也从侧面说明了间接计算法中局域近似对光束的重构只发生在计算$g_{\nu,0}^{(1)}$的过程中。

对图4～图7的场计算结果进行统计分析，考虑到直接法对弱电场无法重构，统计范围仅涉及不小于10^{-7}的电场。表2列出了光束不同离轴距离时的重构场平均误差$\varepsilon_{\mathrm{ave}}^{i}$和平均相对误差$\varepsilon_{\mathrm{rel}}^{i}$，计算公式为

$$\varepsilon_{\mathrm{ave}}^{i}=\frac{1}{N}\sum_{j=1}^{N}\left|\boldsymbol{E}_{i,j}-\boldsymbol{E}_{\mathrm{asr},j}\right| \tag{18}$$

$$\varepsilon_{\mathrm{rel}}^{i}=\frac{1}{N}\sum_{j=1}^{N}\left|\boldsymbol{E}_{i,j}/\boldsymbol{E}_{\mathrm{asr},j}-1\right| \tag{19}$$

式中，角标$i=\mathrm{dir},\mathrm{ind}$代表重构计算方法，角标$j$代表参与统计的场点，$N$表示统计的场点数。可以看出，随着离轴距离增大，直接法与原始场的偏离逐渐递增，而间接法重构误差维持不变。在近轴情况下，直接法与间接法的平均误差$\varepsilon_{\mathrm{ave}}^{i}$比较接近，但相对误差$\varepsilon_{\mathrm{rel}}^{i}$差别明显，这说明二种方法的差异在弱场情况下尤其明显。

表2　重构场效应与离轴距离的关系

Table 2　Dependence of the reconstructed field on the off-axis distance

$\boldsymbol{r}_0(x_0,y_0,z_0)$	Direct method		Indirect method		N
	$\varepsilon_{\mathrm{ave}}^{\mathrm{dir}}$	$\varepsilon_{\mathrm{rel}}^{\mathrm{dir}}$	$\varepsilon_{\mathrm{ave}}^{\mathrm{ind}}$	$\varepsilon_{\mathrm{rel}}^{\mathrm{ind}}$	
(2, 2, 0)	9.47×10^{-5}	0.285	9.42×10^{-5}	9.69×10^{-2}	11 433
(4, 2, 0)	1.12×10^{-4}	0.522			
(6, 2, 0)	1.44×10^{-4}	1.928			
(8, 2, 0)	1.82×10^{-4}	1.785			

图8～图10给出了不同光束束腰半径的重构场比较。光束束腰半径分别为$w_0=3\ \mu\mathrm{m}$、$2\ \mu\mathrm{m}$和$1\ \mu\mathrm{m}$，对应的光束约束参数分别为$s=0.033\,57$、$0.050\,36$和$0.100\,7$。波长$\lambda=0.632\,8\ \mu\mathrm{m}$和光束坐标$(x_0,y_0,z_0)=(1,2,0)\ \mu\mathrm{m}$保持不变。随着束腰半径减小，直接法重构场与原始场的偏离越来越明显，重构场在xy平面内

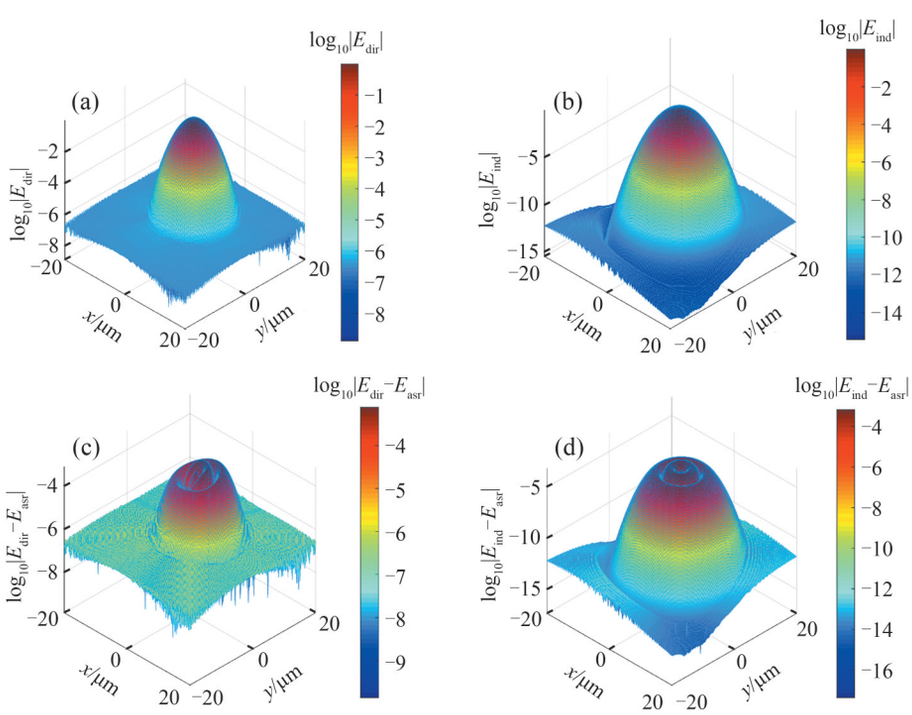

图8　高斯光束的重构场及其偏差，光束束腰半径为$w_0=3\ \mu\mathrm{m}$。(a)直接法重构电场；(b)间接法重构电场；(c)直接法重构误差；(d)间接法重构误差

Fig. 8　Reconstructed electric fields of the Gaussian beam with a waist radius of $w_0=3\ \mu\mathrm{m}$. (a) Electric field reconstructed in direct method; (b) Electric field reconstructed in indirect method; (c) Difference between the original and directly reconstructed fields; (d) Difference between the original and indirectly reconstructed fields

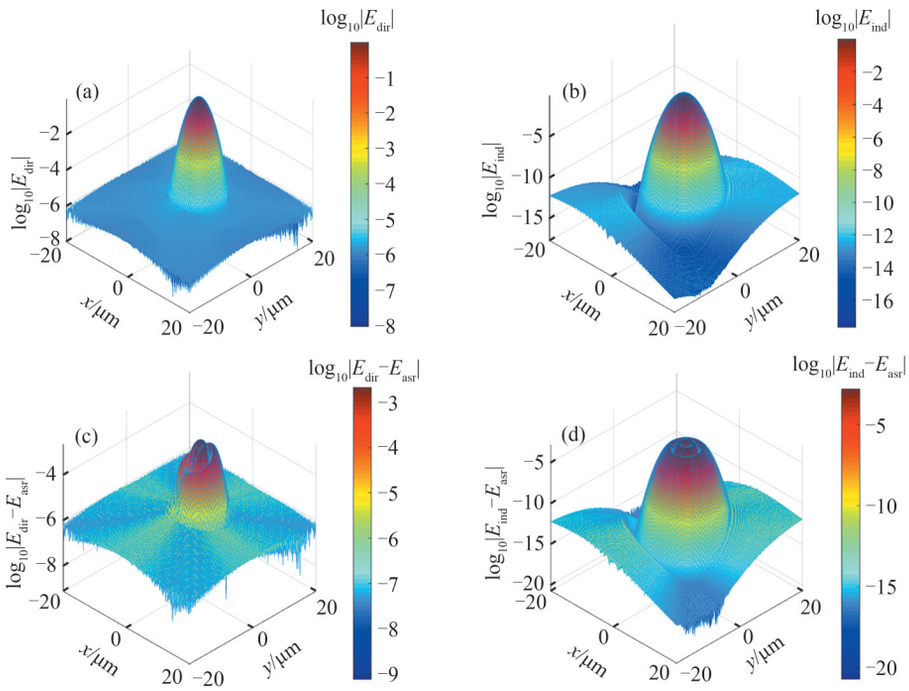

图 9 高斯光束的重构场及其偏差，光束束腰半径为 $w_0=2\ \mu m$。(a)直接法重构电场；(b)间接法重构电场；(c)直接法重构误差；(d)间接法重构误差

Fig. 9 Reconstructed electric fields of the Gaussian beam with a waist radius of $w_0=2\ \mu m$. (a) Electric field reconstructed in direct method; (b) Electric field reconstructed in indirect method; (c) Difference between the original and directly reconstructed fields; (d) Difference between the original and indirectly reconstructed fields

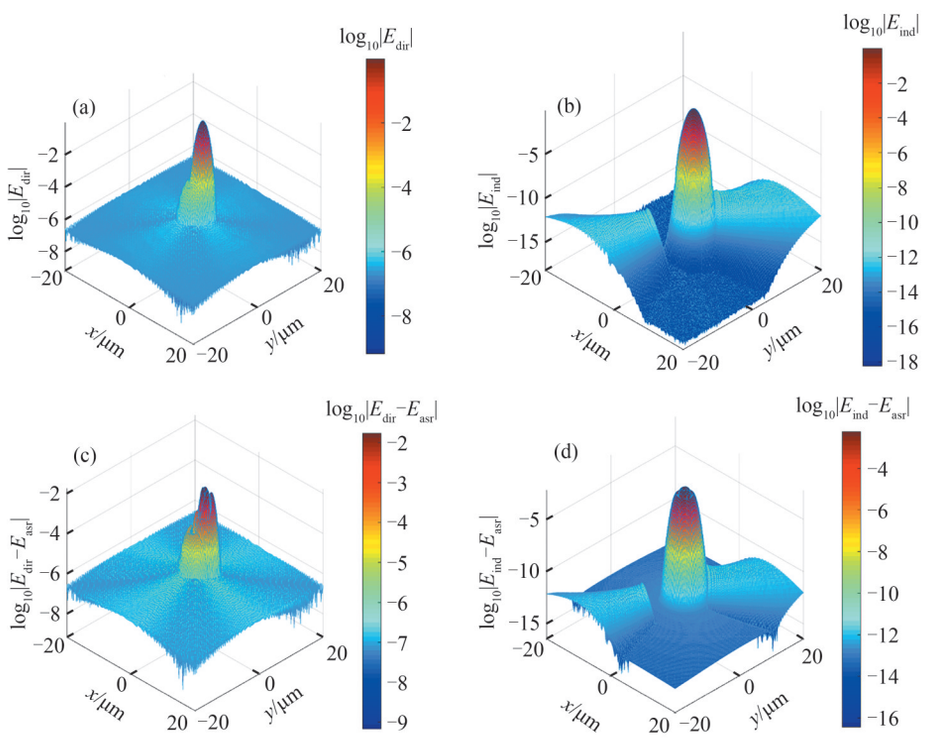

图 10 高斯光束的重构场及其偏差，光束束腰半径为 $w_0=1\ \mu m$。(a)直接法重构电场；(b)间接法重构电场；(c)直接法重构误差；(d)间接法重构误差

Fig. 10 Reconstructed electric fields of the Gaussian beam with a waist radius of $w_0=1\ \mu m$. (a) Electric field reconstructed in direct method; (b) Electric field reconstructed in indirect method; (c) Difference between the original and directly reconstructed fields; (d) Difference between the original and indirectly reconstructed fields

的分布呈现出明显的不对称。重构场与原始场之差的最大值逐渐增大，依次为$\Delta|\boldsymbol{E}|\approx 7.77\times10^{-4}$、$2.16\times10^{-3}$和$1.74\times10^{-2}$。间接法重构场随光束束腰半径的变化情况类似，重构场与原始场之差的最大值逐渐增大，依次为$\Delta|\boldsymbol{E}|\approx 6.69\times10^{-4}$、$1.50\times10^{-3}$和$5.93\times10^{-3}$。显然，与直接法相比较，间接法更接近原始场。而且，间接法所得到的重构场始终保持了高斯光束的轴对称性质。此外，从图8～图10中还可以看到，直接法无法重构出$|\boldsymbol{E}|\leqslant10^{-7}$的场，而间接法的重构场达到$|\boldsymbol{E}|\approx10^{-11}$。这说明，无论是直接法还是间接法，其重构效果都与光束的会聚情况有关。当光束束腰半径较大（光束会聚较弱）时，局域近似法得到的计算结果更加接近原始场；反之当光束束腰半径较小（光束会聚较强）时，局域近似法得到的计算结果严重偏离原始场。该结果与文献[40]的结论吻合。表3给出了不同束腰情况下的误差分析，可以看出随着束腰半径减小，二种计算方法所得到的重构场与原始场的偏离度都在增大。这说明局域近似法对强会聚高斯光束并不适用。一般来说局域近似法只适用于$w_0>\lambda$（或$s\leqslant0.1$）的情况，在重构要求较高（较小的重构误差）的情况下应满足$w_0\gg\lambda$。

表3　重构场效应与光束束腰的关系

Table 3　Dependence of the reconstructed field on the beam waist radius.

w_0	Direct method		Indirect method		N
	$\varepsilon_{\mathrm{ave}}^{\mathrm{dir}}$	$\varepsilon_{\mathrm{rel}}^{\mathrm{dir}}$	$\varepsilon_{\mathrm{ave}}^{\mathrm{ind}}$	$\varepsilon_{\mathrm{rel}}^{\mathrm{ind}}$	
1	1.33×10^{-3}	19.61	8.22×10^{-4}	0.525	1 101
2	2.20×10^{-4}	1.130	2.11×10^{-4}	0.201	4 381
3	9.29×10^{-5}	0.248	9.42×10^{-5}	9.69×10^{-2}	9 777

总体而言，从直接法和间接法之间的比较可以发现，间接计算方法比直接计算方法具有明显的优势。首先，间接法能够重构出更弱的场分布，而且重构场保持了高斯光束的轴对称分布；其次，间接法与光束的离轴距离不敏感，可以在较大的离轴情况下使用；再次，在强会聚情况下，间接法能得到比直接法更加接近原始场的重构分布；最后，间接法在计算电磁场的光束形状系数时体现出更快的运算速度。

3　结论

本文采用两步间接法结合局域近似法计算高斯光束的光束形状系数，并与直接计算方法进行比较。在间接计算方法中，只需要推导光束中心位于坐标系原点时标量光束形状系数的表达式并编程。标量光束形状系数的平移计算以及向矢量光束形状系数的转化适用于各种光束。因此，间接计算方法在公式的推导和编程方面都更加简单。

数值计算表明：首先，在计算速度方面间接法计算光束形状系数比直接算法快了大约8倍，因此其效率更高。其次，间接计算方法所得结果与光束的离轴距离不敏感，在不同离轴距离下重构场始终保持了高斯光束的轴对称分布，重构场和原始场的差别与离轴距离的大小无关。而直接计算方法与光束离轴距离的关联性较强，当光束离轴距离增大时，重构场越来越偏离对称分布，它与原始场的偏离逐渐增大。当光束离轴距离增大到一定程度时，直接法的重构场中出现了环状的强度约为10^{-5}的伪结构。最后，两种计算方法的重构效果均与光束束腰半径有关。对于弱会聚高斯光束，重构场与原始场比较接近。但随着束腰半径减小，重构场与原始场的偏差逐渐增大。这体现出局域近似法在处理强会聚光束时的局限性。一般而言，无论是直接法还是间接法，光束束腰半径至少不能小于入射光波长。

总体而言，与直接算法相比较，间接法在公式推导和编程方面更加简便，在计算效率上和场重构质量上更优。

参考文献

[1] GOUESBET G，GRÉHAN G. Generalized Lorenz-Mie theories[M]. 3rd Ed. Heidelberg：Springer，2023.

[2] GOUESBET G，LETELLIER C，REN K F，et al. Discussion of two quadrature methods of evaluating beam-shape coefficients in generalized Lorenz-Mie theory[J]. Applied Optics，1996，35(9)：1537-1542.

[3] GOUESBET G，AMBROSIO L A，LOCK J A. On an infinite number of quadratures to evaluate beam shape coefficients in generalized Lorenz-Mie theory and the extended boundary condition method for structured EM beams[J]. Journal of Quantitative Spectroscopy and Radiative Transfer，2020，242：106779.

[4] GOUESBET G, GRÉHAN G, MAHEU B. On the generalized Lorenz-Mie theory: first attempt to design a localized approximation to the computation of the coefficients gn[J]. Journal of Optics, 1989, 20(1): 31-43.
[5] GOUESBET G, GRÉHAN G, MAHEU B. Localized interpretation to compute all the coefficients g_n in the generalized Lorenz-Mie theory[J]. Journal of the Optical Society of America A, 1990, 7(6): 998-1007.
[6] REN K F, GOUESBET G, GRÉHAN G. Integral localized approximation in generalized Lorenz-Mie theory[J]. Applied Optics, 1998, 37(19): 4218-4225.
[7] GOUESBET G, GRÉHAN G, MAHEU B. Computations of the g_n coefficients in the generalized Lorenz-Mie theory using three different methods [J]. Applied Optics, 1988, 27(23): 4874-4883.
[8] GOUESBET G, GRÉHAN G, MAHEU B. Expressions to compute the coefficients g_n^m in the generalized Lorenz-Mie theory using finite series [J]. Journal of Optics, 1988, 19(1): 35-48.
[9] AMBROSIO L A, GOUESBET G. Modified finite series technique for the evaluation of beam shape coefficients in the T-matrix methods for structured beams with application to Bessel beams [J]. Journal of Quantitative Spectroscopy and Radiative Transfer, 2020, 248: 107007.
[10] GOUESBET G, LOCK J A, HAN Y, et al. Efficient computation of arbitrary beam scattering on a sphere: Comments and rebuttal, with a review on the angular spectrum decomposition[J]. Journal of Quantitative Spectroscopy and Radiative Transfer, 2021, 276: 107913.
[11] DOICU A, WRIEDT T. Plane wave spectrum of electromagnetic beams [J]. Optics Communications, 1997, 136: 114-124.
[12] SHEN Jianqi, WANG Ying, YU Haitao, et al. Angular spectrum representation of the Bessel-Gauss beam and its approximation: A comparison with the localized approximation [J]. Journal of Quantitative Spectroscopy and Radiative Transfer, 2022, 284: 108167.
[13] VALDIVIA N L, AMBROSIO L A. Bessel-Gauss description in the generalized Lorenz-Mie theory: the finite series method[C]. IEEE MTT-S International Microwave and Optoelectronics Conference (IMOC),2019.
[14] GOUESBET G, VOTTO L F M, AMBROSIO L A. Finite series expressions to evaluate the beam shape coefficients of a Laguerre-Gauss beam freely propagating[J]. Journal of Quantitative Spectroscopy and Radiative Transfer, 2019, 227: 12-19.
[15] VOTTO L F M, AMBROSIO L A, GOUESBET G. Evaluation of beam shape coefficients of paraxial Laguerre-Gauss beam freely propagating by using three remodeling methods [J]. Journal of Quantitative Spectroscopy and Radiative Transfer, 2019, 239: 106618.
[16] VAN DE HULST H C. Light scattering by small particles[M]. New York: Dover, 1981: 208-210.
[17] GOUESBET G, VOTTO L F M, AMBROSIO L A. Finite series expressions to evaluate the beam shape coefficients of a Laguerre-Gauss beam freely propagating[J]. Journal of Quantitative Spectroscopy and Radiative Transfer, 2019, 227: 12-19.
[18] GOUESBET G, AMBROSIO L A, VOTTO L F M. Finite series expressions to evaluate the beam shape coefficients of a Laguerre-Gauss beam focused by a lens in an on-axis configuration [J]. Journal of Quantitative Spectroscopy and Radiative Transfer, 2019, 242: 106759.
[19] VALDIVIA N L, VOTTO L F M, GOUESBET G, et al. Bessel-Gauss beams in the generalized Lorenz-Mie theory using three remodeling techniques[J]. Journal of Quantitative Spectroscopy and Radiative Transfer, 2020, 256:107292.
[20] VOTTO L F M, AMBROSIO L A, GOUESBET G, et al. Finite series algorithm design for lens-focused Laguerre-Gauss beams in the generalized Lorenz-Mie theory [J]. Journal of Quantitative Spectroscopy and Radiative Transfer, 2021, 261: 107488.
[21] VOTTO L F M, CHAFIQ A, BELAFHAL A, et al. Hermite-Gaussian beams in the generalized Lorenz-Mie theory through finite-series Laguerre-Gaussian beam shape coefficients[J]. Journal of the Optical Society of America B, 2022, 39(4): 1027-1032.
[22] VOTTO L F M, CHAFIQ A, GOUESBET G, et al. Ince-Gaussian beams in the generalized Lorenz-Mie theory through finite series Laguerre-Gaussian beam shape coefficients [J]. Journal of Quantitative Spectroscopy and Radiative Transfer, 2023, 302: 108565.
[23] VOTTO L F M, GOUESBET G, AMBROSIO L A. A framework for the finite series method of the generalized Lorenz-Mie theory and its application to freely propagating Laguerre-Gaussian beams[J]. Journal of Quantitative Spectroscopy and Radiative Transfer, 2023, 309:108706.
[24] LOCK J A, GOUESBET G. Rigorous justification of the localized approximation to the beam-shape coefficients in generalized Lorenz-Mie theory. II. Off-axis beams[J]. Journal of the Optical Society of America A, 1994, 11(9): 2516-2525.
[25] SHEN Jianqi, JIA Xiaowei, YU Haitao. Compact formulation of the beam shape coefficients for elliptical Gaussian beam based on localized approximation[J]. Journal of the Optical Society of America A, 2016, 33(11):2256-2263.

[26] JIA Xiaowei, SHEN Jianqi, YU Haitao. Calculation of generalized Lorenz-Mie theory based on the localized beam models[J]. Journal of Quantitative Spectroscopy and Radiative Transfer, 2017, 195: 44-54.
[27] QIU Juncheng, SHEN Jianqi. Beam shape coefficient calculation for a Gaussian beam: localized approximation, quadrature and angular spectrum decomposition methods[J]. Applied Optics, 2018, 57(2): 302-313.
[28] WANG Wei, SHEN Jianqi. Beam shape coefficients calculation for an elliptical Gaussian beam with 1-dimensional quadrature and localized approximation methods[J]. Journal of Quantitative Spectroscopy and Radiative Transfer, 2018, 212: 139-148.
[29] SHEN Jianqi, LIU Xiang, WANG Wei, et al. Calculation of light scattering of an elliptical Gaussian beam by a spherical particle[J]. Journal of the Optical Society of America A, 2018, 35(8):1288-1298.
[30] SHEN Jianqi, WANG Yu, ZHONG Shiliang, et al. Speed up the beam shape coefficient evaluation by using scalar spherical wave expansion and scalar translational addition theorem[J]. Journal of Quantitative Spectroscopy and Radiative Transfer, 2025, 334: 109343.
[31] SHEN Jianqi, ZHONG Siliang, LIN Jianxin. Formulation of the beam shape coefficients based on spherical expansion of the scalar function[J]. Journal of Quantitative Spectroscopy and Radiative Transfer, 2023, 309: 108705.
[32] STRATTON J A. Electromagnetic Theory[M]. New York: McGraw-Hill, 1941: 349-423.
[33] FRIEDMAN B, RUSSEK J. Addition theorems for spherical waves[J]. Quarterly of Applied Mathematics, 1954, 12(1): 13-23.
[34] STEIN S. Addition theorems for spherical wave functions[J]. Quarterly of Applied Mathematics, 1961, 19(1): 15-24.
[35] CRUZAN O R. Translational addition theorems for spherical vector wave functions[J]. Quarterly of Applied Mathematics, 1962, 20(1): 33-40.
[36] CHEW W C. Recurrence relations for three-dimensional scalar addition theorem[J]. Journal of Electromagnetic Waves and Applications, 1992, 6(1-4): 133-142.
[37] TANG Siqi, SHEN Jianqi, WANG Mengyang. Angular spectrum decomposition method for evaluating the beam shape coefficients of the scalar Gaussian beams with two approaches in approximation[J]. Optics Express, 2025, 33(6): 14061-14082.
[38] MISHRA S R. A vector wave analysis of a Bessel beam[J]. Optics Communications, 1991, 85: 159-161.
[39] ZHONG Shiliang, LIN Jianxin, SHEN Jianqi. Beam shape coefficients of hollow vortex Gaussian beam and near-field scattering[J]. Journal of the Optical Society of America A, 2024, 41(7): 1403-1412.
[40] LOCK J A, GOUESBET G. Rigorous justification of the localized approximation to the beam-shape coefficients in generalized Lorenz-Mie theory. I. On-axis beams[J]. Journal of the Optical Society of America A, 1994, 11(9): 2503-2515.

Remodeling of the Localized Approximation: Beam Shape Coefficient Calculation for the Gaussian Beam by Using Scalar Translation Addition Theorem

WANG Yu, TIAN Yiqian, JIANG Haoyu, SHEN Jianqi
(*College of Science, University of Shanghai for Science and Technology, Shanghai* 200093, *China*)

Abstract: The accurate and efficient calculation of the Beam Shape Coefficients (BSCs) is one of the key issues in researching the interaction between a structured or shaped beam and the particles. For this reason, different techniques have been established, such as the quadrature method, the Localized Approximation (LA) or its variants, the Finite Series (FS) method, the Angular Spectrum Decomposition (ASD), and the others. Among these methods, the Localized approximation has been widely used due to its advantages including mainly the efficiency in numerical calculation, the conciseness of the expressions and the straightforwardness in deducing the BSCs for the beams in both the on-axis and off-axis scenarios. However, this method, just as it is named, is an approximate one. The beam remodeling takes place when the beam field is reconstructed from the BSCs, i.e. the reconstructed beam field deviates from the originally given field. Up to date, the remodeling of the beam field has not been studied systematically.

In this work, the two-step indirect method is employed to study the remodeling effects of the localized approximation method for the Gaussian beams. In the first step, the expression of the BSCs is obtained, by

using the localized approximation, for the Gaussian beam which is centered in the coordinate system (called beam system) and is described by using a scalar potential function (therefore the BSCs are called scalar BSCs). Subsequently, the scalar translational addition theorem is used to transform the BSCs into another coordinate system whose axes are parallel to those of the beam system. The second coordinate system in which the spherical particle is centered is called particle system. In the second step of the indirect method, the electric and magnetic (EM) fields of the Gaussian beam are described by using the scalar potential function together with a polarization parameter. Based on this relation, the BSCs of the EM field (called vector BSCs or EM BSCs) are expressed as a linear combination of the scalar BSCs. In this way, the EM BSCs for the off-axis located Gaussian beam are obtained indirectly from the scalar BSCs of the centered beam. The two-step indirect method simplifies the analytical derivation of the BSCs. The expressions of the EM BSCs which are directly deduced in the localized approximation for the off-axis located Gaussian beam are used in the numerical calculations for making a comparison. It is found that the indirect method is at least eight times faster than the direct method in numerical calculation of the BSCs.

The remodeling of the localized approximation is studied, based on a comparison between the originally given field of the Gaussian beam and the fields which are reconstructed from the directly and/or indirectly calculated EM BSCs. The numerical results reveal that, in the direct LA method, the axisymmetric structure of the Gaussian beam is broken in the reconstructed beam field, exhibiting spurious-peaks in the electric field. When the off-axis distance becomes sufficiently large, a ring structure is produced in the field. The deviation of the reconstructed beam field from the given one increases gradually along the increase of the off-axis distance. However, in the indirect method, the reconstructed field is always axisymmetric and the discrepancy between the reconstructed and given fields is independent of the off-axis distance. In both the direct and indirect methods, the reconstructed beam fields deviate from the given one, showing a close dependence on the beam waist radius. Namely, the reconstructed beam fields agree much better with the given field when the beam waist radius is large, but the quality of the remodeled fields become poorer when the beam waist radius decreases, especially when the beam waist radius is close to or less than the wavelength of the light beam.

It is concluded that, compared with the direct localized approximation method, the two-step indirect method has advantages in analytical derivation of the BSCs, in conciseness of the expressions, in efficiency of numerical calculation, and in quality of reconstructed beam field. Besides, the work presented here suggests a warning against the use of the direct/indirect LA methods for strongly focused Gaussian beams and the use of the direct LA for large off-axis located beams.

Key words: Beam shape coefficient; Scalar translational addition theorem; Local approximation; Gaussian beam; Beam remodeling

OCIS Codes: 290.5825; 290.4020; 260.0260; 140.3295

CSTR: 32255.14.gzxb20265503.0326002